Int. J. Electrochem. Sci., 6 **(2011)** 4388 - 4403

International Journal of
ELECTROCHEMICAL
SCIENCE
www.electrochemsci.org

Nitrite Electrochemical Sensor Based on Prussian Blue /Single-Walled Carbon Nanotubes Modified Pyrolytic Graphite Electrode.

Abolanle S. Adekunle[1,2], *Bhekie B. Mamba*[1], *Bolade O. Agboola*[3,*], *Kenneth I. Ozoemena*[4]

[1] Department of Chemical Technology, University of Johannesburg, P.O. Box 17011, Doornfontein, 2028, South Africa
[2] Department of Chemistry, Obafemi Awolowo University, Ile-Ife, Nigeria
[3] Department of Petroleum Chemistry and Engineering, American University of Nigeria, Yola, Nigeria
[4] Energy & Processes Unit, Materials Science and Manufacturing, Council for Scientific and Industrial Research (CSIR), Pretoria 0001, South Africa
[*]E-mail: bolade_agboola@yahoo.co.uk

Received: 3 July 2011 / *Accepted:* 15 August 2011 / *Published:* 1 September 2011

Nitrite, NO_2^- (in neutral), and NO (in acidic media) were used as analytical probe to investigate the electrocatalytic properties of Prussian blue nanoparticles (PB) modified edge plane pyrolytic graphite (EPPG) electrode. Results indicate that single-walled carbon nanotubes-Prussian blue hybrid (SWCNT-PB) modified electrode demonstrated greater sensitivity and catalysis towards nitrite compared to PB or a SWCNT modified electrode. The current response of the electrode was reduced in the presence of cetyltrimethylammoniumbromide (CTAB) which was used as a stabilising agent. Electrocatalytic oxidation of nitrite occurred through a simple adsorption controlled electrode reaction. The adsorption equilibrium constant β and the standard free energy change ΔG^0 due to adsorption were 4.35 x 10^3 $M^{-1}s^{-1}$ (-20.76 $kJmol^{-1}$) and 15.0 x 10^4 $M^{-1}s^{-1}$ (-29.53 $kJmol^{-1}$) for nitrite and nitric oxide respectively. Despite the adsorption, the EPPGE-SWCNT-PB electrode showed good stability of greater than 80% in the analytes. The electrode's limit of detection and catalytic rate constant were 6.26 µM (4.37 x 10^6 cm^3 mol^{-1} s^{-1}) and 4.9 µM (6.35 x 10^5 $cm^3mol^{-1}s^{-1}$) for nitrite and nitric oxide respectively. The fabricated electrode is not difficult to prepare and could serve as a potential sensor for nitrite determination in food and environmental samples.

Keywords: Single-walled carbon nanotubes; Edge plane pyrolytic graphite electrode; Prussian blue nanoparticles; Oxidation; Nitrite; Adsorption.

1. INTRODUCTION

Environmentally important molecules such as nitrites have attracted the attention of analytical chemists and electrochemist in recent times [1-7]. The nitrite ion is an intermediate species in the

nitrogen cycle, resulting from the oxidation of ammonia or from reduction of nitrate [4]. It is used as an additive in some types of food and its occurrence in soils, waters, foods and physiological systems is prevalent [2]. The nitrite ion is classified as an environmentally hazardous species because of its toxicity [8] and combines with blood pigments to produce meta-haemoglobin which leads to oxygen depletion to the tissues [3,4]. Upon combining in the stomach with amines and amides highly carcinogenic N-nitrosamine compounds are produced [9]. Thus, there is need for the detection and quantification of the nitrite anion using simple, effective and less expensive analytical techniques.

The desired redox reaction at the bare electrode using voltammetric techniques such as cyclic voltammetry (CV) and square wave voltammetry (SWV) often involves slow transfer kinetics and therefore occurs at an appreciable rate only at a potential substantially higher than its thermodynamic redox potential. Such reactions can be catalysed by attaching to the surface a suitable electron-transfer mediator. The function of the mediator is to facilitate the charge transfer between the analyte and the electrode. Carbon electrodes (such as the glassy carbon, carbon paste, highly oriented pyrolytic graphite, basal plane pyrolytic graphite and edge plane pyrolytic graphites electrodes) have long been recognized as versatile and supporting platforms for electrocatalysis and electrochemical sensing due to their numerous advantages such as low cost, chemical inertness and wide potential window applicability in most electrolyte solutions compared to precious metal electrodes such as gold, platinum, aluminium, silver and copper. Among the carbon based electrodes, the edged plane pyrolytic graphite electrodes (EPPGE) are reported to have better catalytic activity and reactivity which is mainly due to edge plane sites/defects which are key to fast heterogeneous charge transfer [10] and the EPPGE electrode was therefore chosen for this study. The application of EPPG electrode includes the detection of NADH [11], chlorine [12], halides [13], ascorbic acid [14], cathodic stripping voltammetry of manganese [15] and anodic stripping voltammetry of silver [16].

The application of Prussian blue nanocomposites with dendrimers in the electrochemical detection of dopamine and hydrogen peroxide has been well illustrated [17]. Also, prussian blue (PB) ($Fe_4(III)[Fe(II)(CN)_6]_3$) have found applications in fuel cell devices [18] and as PB–based carbon paste electrode in biosensors [19]. Properties of CNTs have been widely reported and single-walled carbon nanotubes (SWCNTs) possess important mechanical, thermal, photochemical and electrical properties [20] which are industrially useful. In addition, nitrite or nitric oxide detection and quantification have been carried out using sensors incorporating CNT as part of the electrode materials [21, 22]. Therefore, this study exploits the unique properties of SWCNT-PB nanocomposite acting as electron-transfer mediator between the base EPPG electrode and nitrite during electrocatalytic oxidation of nitrite. The electrochemical technique for sensing was chosen in this work because of its fast reaction kinetics, reproducibility of results and stability over the conventional analytical techniques such as spectrophotometry [23], chromatography [24], and flourimetry methods of analysis which are time consuming and sometimes require complex derivatization procedures.

Herein, we report on the electrocatalytic detection of nitrite and its reaction mechanism at the EPPGE modified electrode with or without single SWCNT and PB nanoparticles. The analytes demonstrated some degree of adsorption and signal recovery, which measures the level of stability of the electroactive material on the electrode. The low limit of detection, sensitivity and easy modification of the electrode with the PB nanoparticles is much cheaper and can be readily available

for commercial application. These are some of the advantages of the fabricated sensor over previous reports in the literature.

2. EXPERIMENTAL

2.1 Materials and Reagents

A polyaminobenzene sulphonated single-walled carbon nanotubes (SWCNT-PABS) was purchased from Aldrich and was used directly without further treatment. $FeCl_3$, $K_4[Fe(CN)_6].6H_20$, KCl, diethylaminoethanethiol (DEAET), sodium nitrite, cetyltrimethylammoniumbromide (CTAB) and other chemicals and reagents were of analytical grade and purchased from Sigma-Aldrich chemicals.

Ultra pure water of resistivity 18.2 MΩ was obtained from a Milli-Q Water System (Millipore Corp., Bedford, MA, USA) and was used throughout for the preparation of solutions. A phosphate buffer solution (PBS) of pH 3.0, 7.0 and 7.4 was prepared with appropriate amounts of $NaH_2PO_4.2H_2O$ and $Na_2HPO4.2H_2O$, and adjusted with 0.1 M H_3PO_4 or NaOH. Prepared solutions were purged with pure nitrogen to eliminate oxygen and prevent any form of external oxidation during every electrochemical experiment.

2.2 Equipment and Procedure

The edge plane pyrolytic graphite electrode plate (3mm diameter) was purchased from Le Carbone, Sussex, UK and was constructed locally by placing it in a teflon tube, extended outside with a copper wire to make electrical contact with the electrochemical equipment. Field emission scanning electron microscopy (FESEM) images were obtained from JEOL JSM 5800 LV (Japan). The Transmission electron microscopy (TEM) experiment was performed with the help of a Model JEOL JEM-2100F, Tokyo (Japan), while the energy dispersive x-ray spectra (EDS) were obtained from NORAN VANTAGE (USA).

Electrochemical experiments were carried out using an Autolab Potentiostat PGSTAT 302 (Eco Chemie, Utrecht, and The Netherlands) driven by the GPES software version 4.9. Electrochemical impedance spectroscopy (EIS) measurements were performed with Autolab Frequency Response Analyser (FRA) software between 10 kHz and 10 mHz using a 5 mV rms sinusoidal modulation with the solution of the analyte at their respective peak potential of oxidation (vs. Ag|AgCl in sat. KCl). A Ag|AgCl in saturated KCl and platinum wire were used as reference and counter electrodes respectively.

A bench top pH / ISE ORION meter, model 420A, was used for pH measurements. All experiments were performed at 25 ± 1 °C while the solutions were de-aerated before every electrochemical experiment.

2.3 Electrode modification procedure

EPPGE surface was cleaned by gentle polishing in aqueous slurry of alumina nanopowder (Sigma-Aldrich) on a SiC-emery paper followed by a mirror finish on a Buehler felt pad. The electrode was then subjected to ultrasonic vibration in absolute ethanol to remove residual alumina particles that might be trapped on the surface. EPPGE-SWCNT or EPPGE-CTAB-SWCNT was prepared by a drop-dry method. About 10 μL drops of the SWCNT-PABS in H_2O or CTAB solution (0.1 mg SWCNT-PABS in 1 mL H_2O or 1ml CTAB solution) was dropped on the bare EPPGE and dried in an oven at 50 ^oC for 2 mins. PB nanoparticles were deposited on the electrode using a procedure described by Han et al. [25]. The EPPGE-SWCNT or EPPGE-CTAB-SWCNT electrode was immersed in stirred $FeCl_3$ solution for 30mins after which it was rinsed, dried and immersed in $K_4[Fe(CN)_6]$ solution for another 30mins to give the first layer of PB nanoparticles (first deposition cycle). The modified electrode will be written as EPPGE-SWCNT-PB in this paper. The procedure was repeated to obtain both the second and the third layer of PB nanoparticles. The EPPGE-PB electrode was also obtained following the same procedure but without the addition of SWCNTs.

3. RESULTS AND DISCUSSION

3.1. Electrode Characterisation

The electrochemical characterisation of the studied electrodes and the stability of the PB modified electrodes were previously reported at pH 7.0 PBS containing 0.1M KCl [26]. EPPGE-SWCNT-PB was reported to have shown faster electron transfer properties compared to the other electrodes, and the redox active PB nanoparticles were changed to their reduced form. Prussian white (PW) as shown in Equation 1 suggests successful modification of the electrode with PB nanoparticles [26-28]:

$$\underset{\text{PB}}{KFe(III)[Fe(II)(CN)_6]} + e^- + K^+ \longrightarrow \underset{\text{PW}}{K_2Fe(II)[Fe(II)(CN)_6]} \qquad (1)$$

The electrode surface coverage (Γ_{PB}) was estimated to be 4.8 x 10^{-8} mol cm^{-2}. Figure 1 presents the TEM images of PB nanoparticles (Fig. 1A) and SWCNT-PB nano hybrid (Fig. 1B), while Fig. 1C depicts the SEM image of the SWCNT-PB nano hybrid. From the TEM pictures, the PB particles appeared porous, amorphous, evenly distributed along the nanotubes with average particle size of 5-15 nm. The PB particle distribution on the walls of the CNT could be attributed to both electronic (covalent bonding) and ionic interaction between the phenyl ring, NH_2 or the SO_3^{2-} groups of the SWCNT-PABS and the PB ($Fe_4(III)[Fe(II)(CN)_6]_3$) nanoparticles. The SEM image also revealed the PB particles aggregation along the SWCNT tube indicating several layers of the PB nanoparticles coming together as an aggregate through π–π interactions and ionic bonding. It was reported that a 16

nm nanoparticle contains approximately 4000 unit cells, that is 16000 $[Fe(CN)_6]^{4-}$ and 16000 Fe^{III} ions [29].

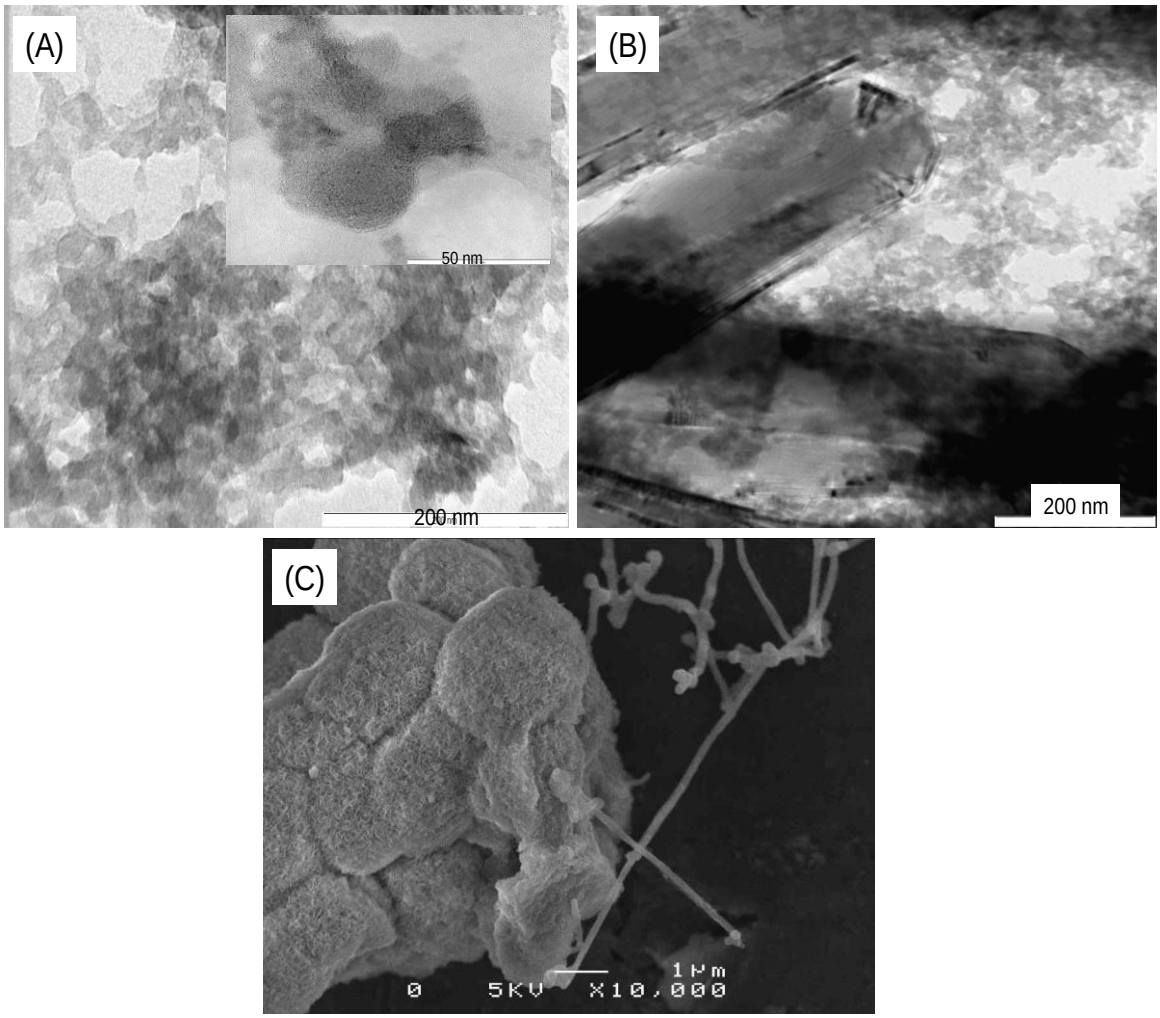

Figure 1. TEM of (a) Prussian blue (PB) nanoparticles (b) SWCNT-PB nano hybrids. (c) is the FESEM images of SWCNT-PB nano hybrids.

3.2 Electrocatalytic oxidation of nitrite

Figures 2 and 3 present the comparative current response of the electrodes towards electro-catalytic oxidation of nitrite (after background current subtraction) at the different pH conditions studied. For example, at pH 7.4 (NO_2^-) and 3.0 (NO) PBS respectively, an irreversible oxidation peak at *ca* 0.8 V corresponding to the oxidation of NO_2^- to NO_3^- through a two (2) electron oxidation process [1,2] or NO to NO_3^- was observed on the bare EPPGE. The 0.8 V (vs. Ag|AgCl, sat'd KCl) or ~ 0.78 V vs SCE) peak potential for nitrite oxidation on bare EPPGE was approximately 200 mV less compared to 0.98 V (vs SCE) peak potential reported for nitrite oxidation on carbon fibre microelectrode CFE [3], and 220 mV less than the peak potential (*ca* 1.0 V vs SCE) for the oxidation of the analyte on bare glassy carbon electrode (GCE) [4,5]. The reduced potential may be due to the fast electron transfer behaviour of the EPPGE itself. However, in comparison to the bare electrode, a

fast electron transfer with a remarkable increase in oxidation current (Figs. 2 and 3) was noticed at the EPPGE-SWCNT-PB electrode.

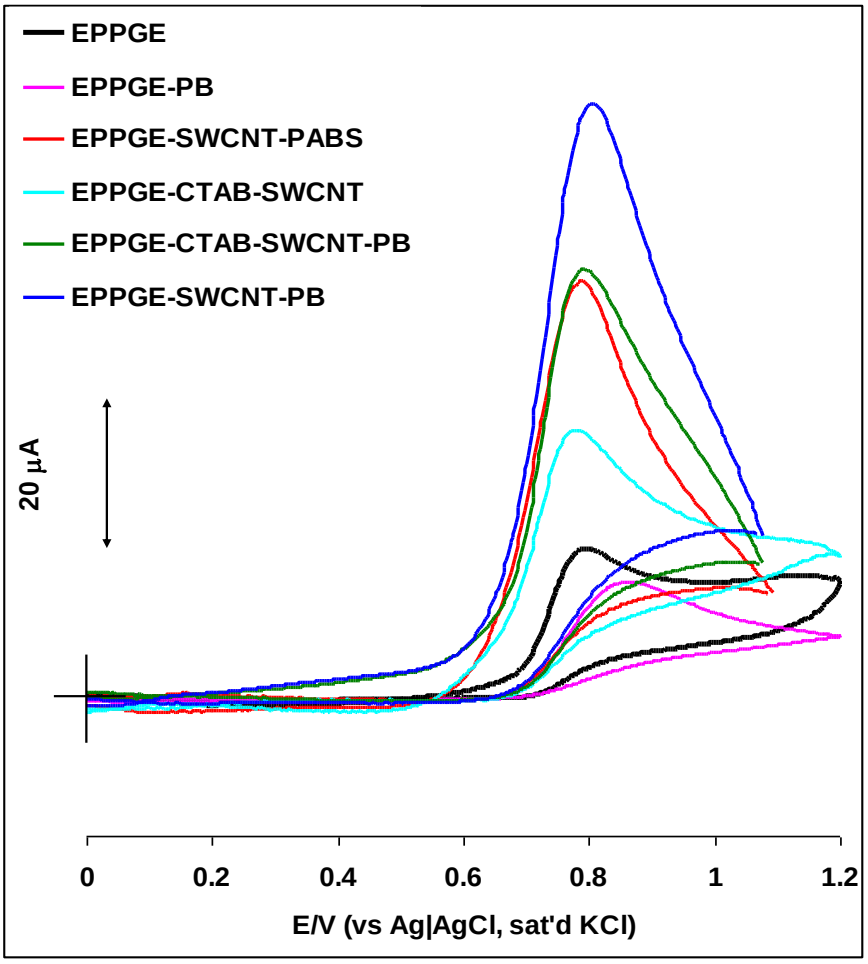

Figure 2. Comparative current response (after background current subtraction) of the bare and the modified electrodes in pH 7.4 PBS containing 10^{-3} M NO_2^- (Scan rate: 25 mVs^{-1}).

In addition, the low on-set potential of catalysis (*ca* 0.54 V) for nitrite oxidation at EPPGE-SWCNT-PB electrode (Fig. 2) compared to other electrodes (0.68 V) also confirmed its superior catalytic efficiency over the other electrodes towards nitrite oxidation. The electrode also demonstrated four time current response (NO_2^-: 87.9 µA, NO: 72.2 µA) compared to the bare EPPGE (NO_2^-: 22.3 µA, NO: 19.8 µA) at both pH studied. Its increasing catalytic activities with increasing PB concentration or PB deposition cycles on the electrode (not shown) makes it the best electrode relative to EPPGE-SWCNT or EPPGE-PB towards nitrite oxidation. The result obtained in this study agreed with a similar observation for nitrite oxidation on gold nanoparticles choline chloride glassy carbon modified electrode (nano-Au/Ch/GCE), which was reported to be better compared to the bare gold, or nano-Au/GCE or Ch/GCE alone [5] signifying the importance of chemically modified electrodes in catalysis. The enhanced performance of the EPPGE-SWCNT-PB electrode has also been attributed to the high surface area coverage of the electroactive SWCNT-PB nanoparticles which was made

possible by the presence of the porous SWCNT layer that allowed more for PB deposition. Due to its excellent electrochemical behaviour, the EPPGE-SWCNT-PB electrode was used for further studies in this work unless otherwise stated.

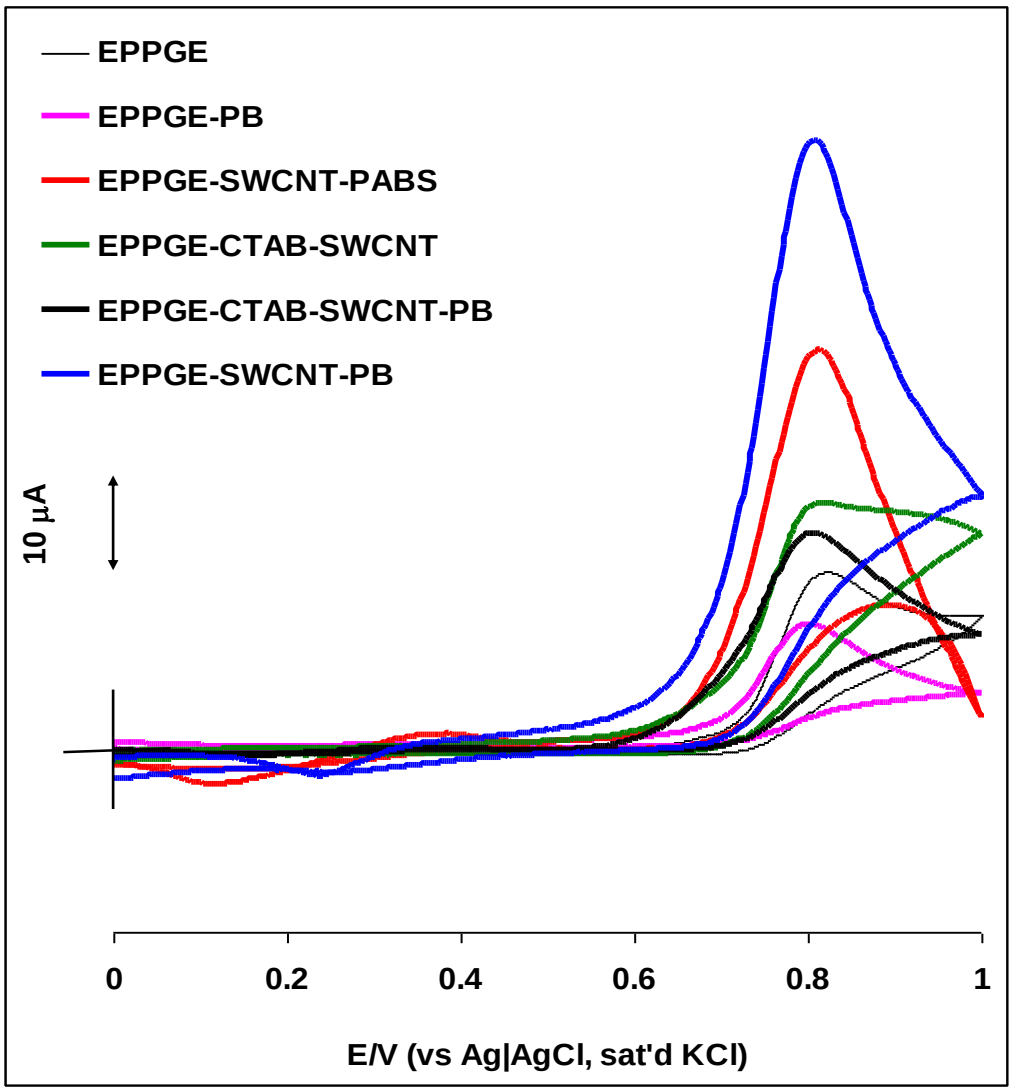

Figure 3. Comparative current response (after background current subtraction) of the bare and the modified electrodes in pH 3.0 PBS containing 10^{-3} M NO (Scan rate: 25 mVs^{-1}).

3.3 Electrochemical impedance studies (Electron transport behaviour)

The electrocatalytic behaviour of nitrite and nitric oxide at EPPGE-SWCNT-PB electrode during electrocatalytic oxidation of the analytes was investigated using the electrochemical impedance spectroscopy (EIS) technique at the peak potential (E_p) where the analytes were best catalysed. The impedance data obtained from the fitting of the EIS spectra for the EPPGE-SWCNT-PB electrode (Figure 4a) is presented in Table 1.

Table 1. Impedance data obtained for the EPPGE-SWCNT-PB modified electrodes in 10^{-3} M nitrite (pH 7.4 PBS) and nitric oxide (pH 3.0 PBS) respectively (at 0.8 V vs Ag|AgCl sat'd KCl). Note that the values in parentheses are percentage errors of the data fitting.

Electrodes	Impedimetric Parameters					
	R_s (Ω cm^2)	CPE (mF)	n	R_{ads} (Ω cm^2)	C_{ads} (μF)	*pseudo* χ^2
	NO_2^-					
EPPGE-SWCNT-PB	14.78 (0.27)	0.08 (6.46)	0.65 (8.54)	2.12 (2.01)	82.40 (5.75)	7.68×10^{-4}
	NO					
EPPGE-SWCNT-PB	17.12 (0.27)	0.16 (5.16)	0.53 (6.61)	4.66 (1.13)	77.0 (4.17)	1.16×10^{-5}

The impedance data was fitted by the electrical circuits (Figure 4b) containing elements represented in Table 1 where R_s is the solution/electrolyte resistance, *CPE* is known as the constant phase element which replaces the true capacitance (C_{dl}), R_{ads} represents the partial charge transfer resistance or resistance due to adsorption, C_{ads} describes the pseudocapacitive nature of the system due to adsorption while n is a function whose value describes the electrical nature of the electrode and has values ($-1 \leq n \leq 1$). $n = 0$ implies pure resistor; $n = 1$, means pure capacitor, $n = -1$ means an inductor; while $n = 0.5$ indicates a Warburg impedance (Z_w) due to diffusion of ions to and from the electrode|solution. A similar circuit was used in the fitting of the impedance data obtained for the other electrodes studied including the bare EPPGE.

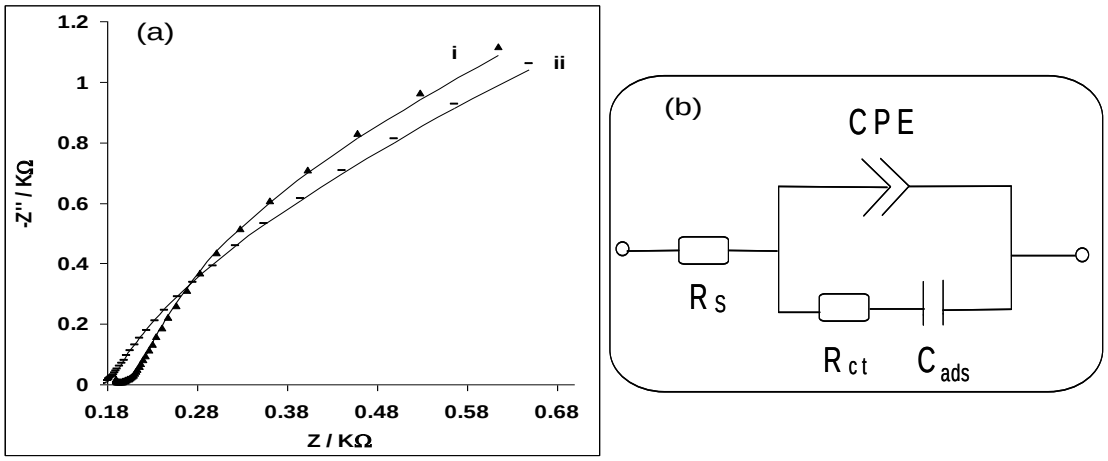

Figure 4. (a) Nyquist plots obtained for the EPPGE-SWCNT-PB electrode in (i) 0.1 M pH 7.4 PBS containing 10^{-3} M NO_2-, and (ii) 0.1 M pH 3.0 PBS containing 10^{-3} M NO. The data points are experimental while the solid lines in the spectra represent non-linear least squares fits. (b) is the circuit diagram used in the fitting of the impedance data in (a).

From Table 1, the R_{ads} of 2.12 and 4.66 Ωcm^2 for the EPPGE-SWCNT-PB electrode in NO_2^- and NO respectively were lower in comparison to 21.05 and 25.42 Ωcm^2 obtained for the bare EPPGE electrode towards the analytes. The result suggests low adsorption of reaction intermediates or oxidation product on the EPPGE-SWCNT-PB electrode, fast electron transport, thus, a more favoured catalysis of the analytes on this electrode compared with the bare EPPGE.

The Bode plots of –phase angle vs. log (f/Hz) (at 0.24 Hz, Fig. 5) obtained for the EPPGE-SWCNT-PB electrode towards the analytes gave a phase angle values of -63.1^0 and -61.2^0 for nitrite and nitric oxide respectively. The analytes behaved similarly towards the electrode, which is pseudocapacitive since a phase angle of -90^0 was expected for a pure capacitive behaviour. Similarly, plots of log |Z/Ω| vs log (f/Hz) (Fig. 5) gave slope values of 0.7321 and 0.6598 for nitrite and nitric oxide respectively, also indicating the pseudocapacitive nature of the electrode towards analytes since for a pure capacitor; a slope value of 1.0 is expected.

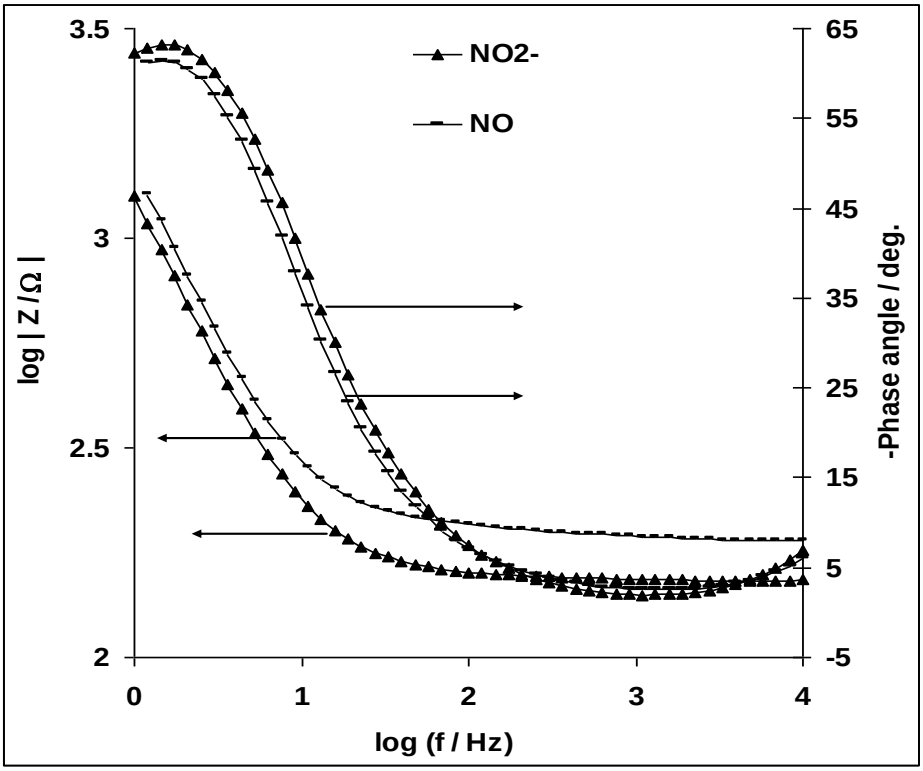

Figure 5. Bode plots of –phase angle/deg, and the log |Z / Ω| vs. log (f / Hz) for the EPPGE-SWCNT-PB electrode in 10^{-3} M NO_2^- and 10^{-3} M NO solutions respectively.

3.4 Stability study

The stability of the EPPGE-SWCNT-PB electrode towards the analyte was studied using cyclic voltammetry experiments by carrying out repetitive (30 scans) cyclic voltammetry in 0.1 M PBS electrolyte as represented by the nitrite ion in Figure 6a. A current drop was observed for the analytes. The drop was associated with adsorption or electrode fouling. However, the electrode was removed

from the solution, cleaned by repetitive scanning in pH 7.0 PBS and re-run in the solution of each analyte.

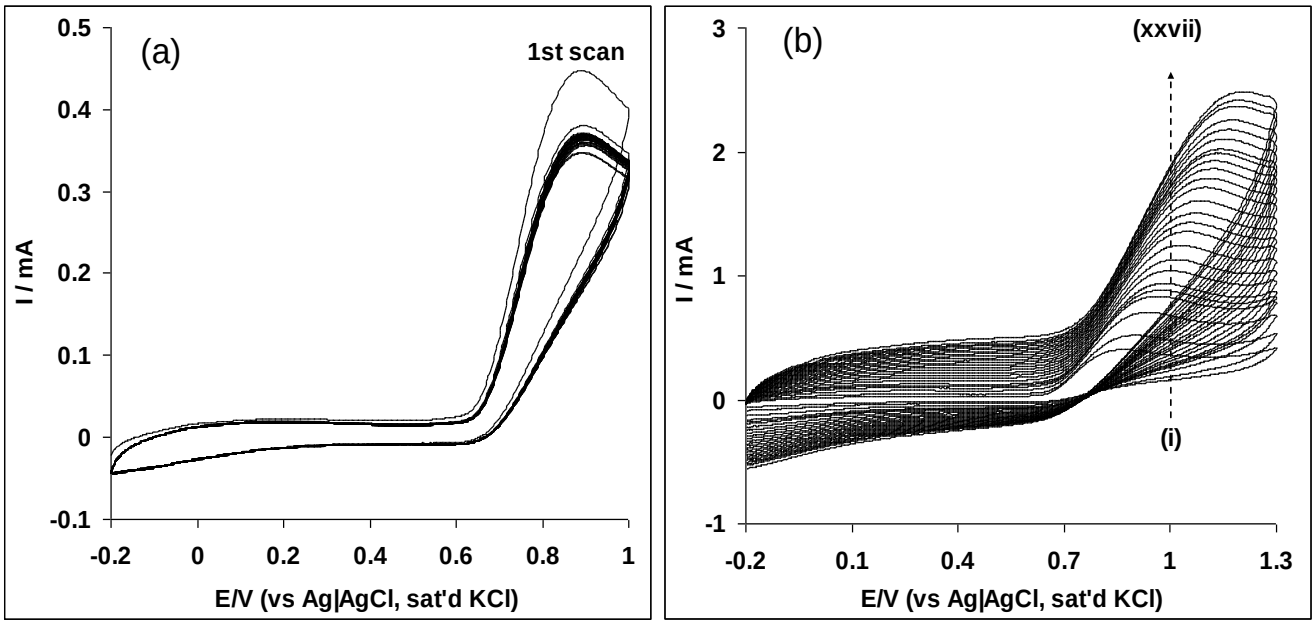

Figure 6. (a) Current response (30 scans) of the EPPGE-SWCNT-PB electrode in pH 7.4 PBS containing 10^{-3} M NO_2^-. (b) Current of the EPPGE-SWCNT-PB 0.1 M pH 7.4 PBS containing 10^{-3} M NO_2^- (scan rate: 25 – 1200 mVs^{-1}, inner to outer).

From the result, 85.0% and 93.7% current recovery were obtained (after electrochemical cleaning) respectively for electro-catalytic oxidation of nitrite and nitric oxide. Therefore, the initial current drop was due to simple physical adsorption of the analyte and can be removed by repetitive cleaning in PBS, and at the same time, the electrode can be re-used for further analysis. Thus, the electrode modifier can be said to be stable and produces a considerable signal or current response if re-used for the electrocatalytic oxidation of the analytes.

3.5 Effect of scan rate

The effect of scan rate (range of 25–1200 mVs^{-1}) was investigated using cyclic voltammetry as shown in Figure 6b. The results reveal that the anodic peak current (I_{pa}) of nitrite oxidation was directly proportional to the square root of scan rate ($\nu^{1/2}$) (R^2 = 0.9914) but the negative intercept suggests that the electrode reaction is not a pure diffusion-controlled process. Randles-Sevčik equation for an anodic oxidation process [30] with a zero intercept suggests a complete diffusion control process, thus, the negative intercept from the plot of I_{pa} versus $\nu^{1/2}$ can be explained as an adsorption of the nitrite molecule after diffusion to the electrode surface, or adsorption of its intermediate or oxidation product after an electrocatalytic process.

Using the Tafel equation for an irreversible-diffusion controlled process [30],

$$Ep = K + \frac{2.303RT}{2(1-\alpha)n_\alpha F}\log \nu \qquad (2)$$

where α is the transfer coefficient, n_α is the number of electrons involved in the rate-determining step. *R*, *T* and *F* are gas constant, temperature and Faraday constant, respectively.

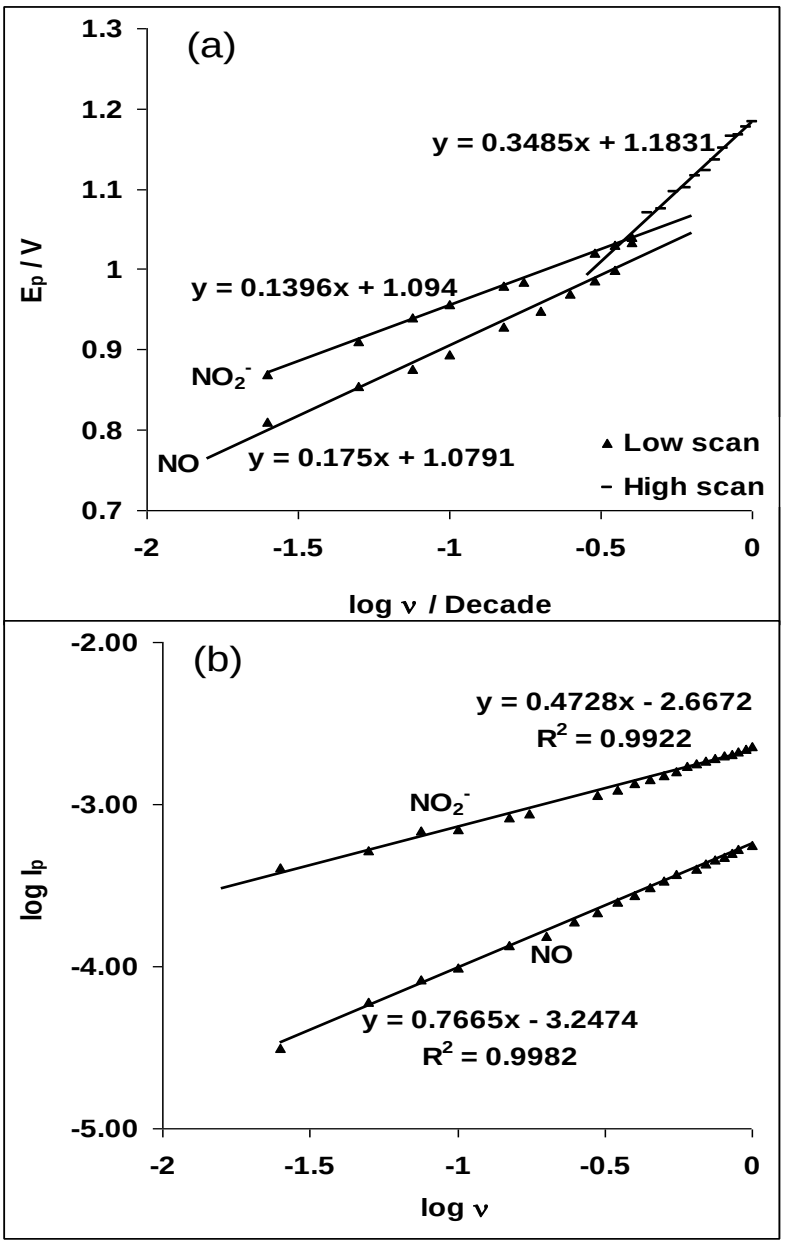

Figure 7. (a) Plots of peak potential (E_p) versus *log* ν for 10^{-3} M NO_2^- and NO respectively. (b) Current function plots of *log* I_p versus *log* ν for 10^{-3} M NO_2^- and 10^{-3} M NO respectively.

A linear plot for E_{pa} vs the log ν was obtained (Fig. 7a). Based on the slope of E_{pa} versus log ν plot, and assuming n_α is 2 for nitrite and nitric oxide [7], the α values were estimated as approximately

0.89 for nitrite at both pH 7.4 and 3.0 PBS respectively. Generally, when an α value is larger than 0.5, this supposed to be a more favoured reaction mechanism [31]. Thus, the high α value obtained in this study for nitrite and nitric oxide further confirms their favoured and excellent electrocatalytic oxidation process on the EPPGE-SWCNT-PB electrode. The 0.89 recorded for nitrite is higher than 0.72 reported recently for the oxidation of the analyte on EPPGE-SWCNT-Co modified electrode [7] or 0.73 reported for its oxidation on cobalt phthalocyanine modified electrode [32]. Also, from the slope of the Tafel plots (E_p vs *log* ν) in Figure 7a, the Tafel slope *b* of 279, 350 $mVdec^{-1}$ at low (25-400 mVs-1) and 697, 819.8 $mVdec^{-1}$ at high scan rate (500-1200 mVs^{-1}) were obtained for NO_2^- and NO respectively. Therefore, irrespective of the scan rate region, the Tafel values obtained in this study further confirm an adsorption process due to the electrocatalytic oxidation of nitrite on the EPPGE-SWCNT-PB electrode. In the same vein, the current function plot of log I_P versus log ν gave slope values of 0.473 and 0.767 for NO_2^- and NO respectively which are lower and higher compared with 0.5 values expected for pure diffusion control electrode process [33].

3.6 Concentration study

The dependence of the EPPGE-SWCNT-PB sensor response on applied potential for amperometric determination of different concentrations of nitrite (0.0, 32.3, 62.5, 118.0, 143.0, 189.0, 211.0 and 250.0 μM) was investigated using chronoamperometric technique at an applied potential of 0.8 V (vs. Ag|AgCl, sat'd KCl). The chronoamperogram (Fig. 8a) was obtained after stirring the mixture thoroughly. The inset in Fig.8a represents the calibration curve for the plot of current against nitrite concentration. The measured peak currents were found to be linear with increasing concentrations. The obtained sensitivity of the sensor was 0.2516 μA/μM (R^2 = 0.9998) for nitrite, and 0.0134 μA/μM (R^2 = 0.9999) for nitric oxide. The detection limit was calculated based on the relationship LoD = 3.3 δ/m [34] where δ is the relative standard deviation of the intercept of the y-coordinates from the line of best fit, and *m* the slope of the same line. The LoD value of 6.26 and 4.9 μM were obtained for nitrite (pH 7.4) and nitric oxide (pH 3.0) respectively. The 6.26 reported for NO_2^- at pH 7.4 agreed closely with 5.61 μM recently reported [7] while the 4.9 μM for NO was lower compared with 8.03 μM also recently reported [7].

From the concentration study above and using Equation 3 [34]:

$$\frac{I_{cat}}{I_L} = \pi^{1/2}\left(kC_o t\right)^{1/2} \qquad (3)$$

where I_{cat} and I_l are the currents in the presence and absence of the analyte, *K* is the catalytic rate constant, C_0 is the bulk concentration and *t* is the elapsed time. From the plot of I_{cat}/I_l vs $t^{1/2}$, the catalytic rate constant *K* for EPPGE-SWCNT-PB in 10^{-3} M NO_2^- and 10^{-3} M NO are 4.37 and 0.64 x 10^6 $cm^3mol^{-1}s^{-1}$. The 4.37 and 0.64 x 10^6 $cm^3mol^{-1}s^{-1}$ obtained for NO_2^- and NO are approximately 137 and 19 folds respectively higher than 0.32 and 0.34 x 10^5 cm^3 mol^{-1} s^{-1} reported for the analytes on EPPGE-SWCNT-Co electrode modified by electrodeposition [7]. The value obtained for nitrite agreed

closely with 2.75 x 10^3 M^{-1} s^{-1} (or 2.75 x 10^6 cm^3 mol^{-1} s^{-1}) reported by Ojani *et. al.*, 2006 [35] for the electrocatalytic reduction of nitrite on carbon paste electrode modified with ferricyanide but lower compared to 7 x 10^5 M^{-1} s^{-1} (or 7 x 10^8 cm^3 mol^{-1} s^{-1}) reported by Trolimova *et. al.*, 2005 [36] for catalytic oxidation of nitric oxide and nitrite by water-soluble manganese (III) meso-tetrakis(*N*-methylpyridinium-4-yl) porphyrin (Mn(III)(4-TMPyP) on indium-tin oxide (ITO) electrode in pH 7.4 phosphate buffer solutions. The difference in magnitude of the *K* value can be due to the different electrode modifier employed in each study.

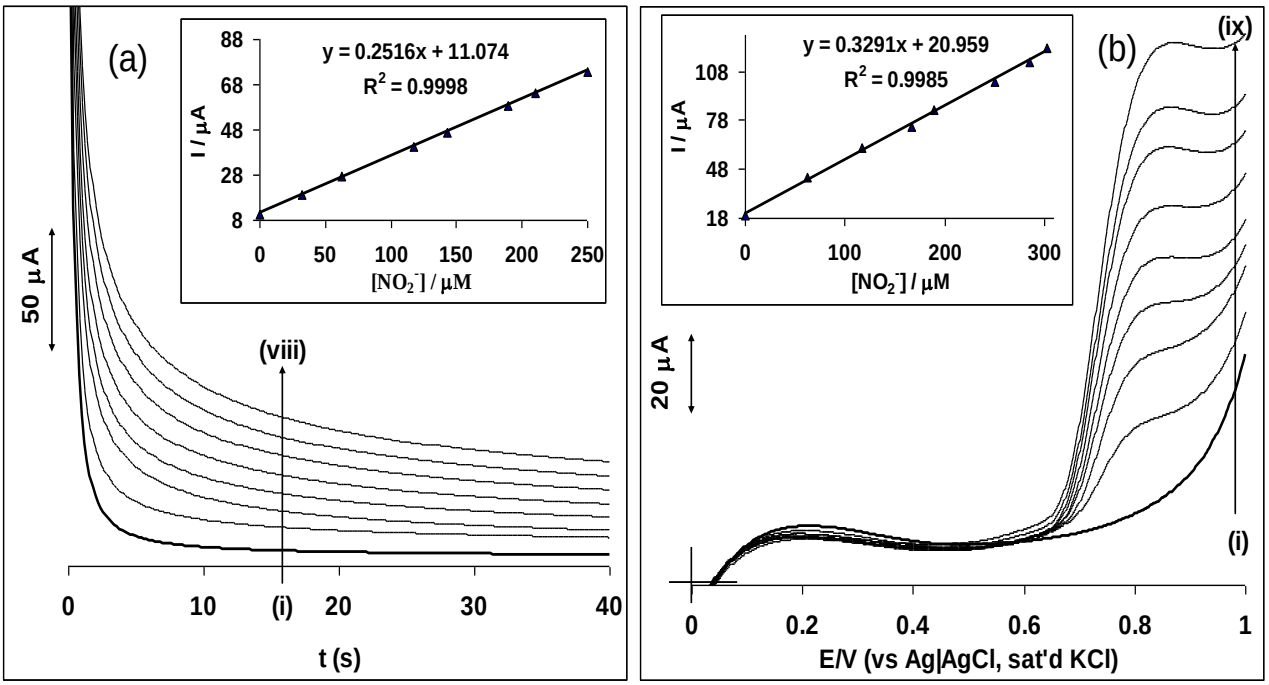

Figure 8. (a) Typical chronoamperogram of EPPGE-SWCNT-PB in pH 7.4 PBS containing different concentrations of Nitrite (0.0, 32.3, 62.5, 118.0, 143.0, 189.0, 211.0 and 250.0 µM (i to viii)). (b) Linear sweep voltammogram of EPPGE-SWCNT-PB in pH 7.4 PBS containing different concentrations of Nitrite (0.0, 32.3, 62.5, 118.0, 167.0, 189.0, 250.0, 285.0 and 302.0 µM (i to ix)). Insets in (a) and (b) are the plots of current response vs nitrite concentration.

3.7 Adsorption controlled electrode reaction

Since the analytes studied adsorbed at different levels on the EPPGE-SWCNT-PB electrode based on their Tafel values, linear sweep or stripping voltammetry (LSV) technique was employed to monitor the extent of adsorption of the analyte on the electrode at different concentrations. Fig. 8b presents the voltammograms obtained for nitrite after allowing the electrode to stir in the analyte for 15 mins. From Langmuir adsorption isotherm theory (Eqn.4, [37]), where I_{cat}, I_{max} and β means catalytic current, maximum current and adsorption equilibrium constant, the plot of the ratio of [Nitrite] / I_{cat} against [Nitrite] gave a straight line (not shown) which confirms an adsorption controlled electrode process.

$$\frac{[\text{Nitrite}]}{I_{cat}} = \frac{I}{\beta I_{max}} + \frac{[\text{Nitrite}]}{I_{max}} \quad (4)$$

From the slope and the intercept of the curve obtained above, the adsorption equilibrium constant β for nitrite and nitric oxide on the electrode was (4.35 ± 0.03) x 10^3 M^{-1} and (15.0 ± 0.03) x 10^4 M^{-1}. From Eqn. 5 below which relates the Gibbs free energy change due to adsorption (ΔG^o) to β, the ΔG^o values were estimated as -20.76 and -29.53 kJmol^{-1} for nitrite and nitric oxide.

$$\Delta G^o = -RTln\beta \quad (5)$$

The -20.76 and -29.53 kJmol^{-1} for nitrite and nitric oxide are higher than -6.36 and -10.0 kJmol^{-1} reported for the analytes on EPPGE-SWCNT-Co modified electrodes [7], thus, validating the high Tafel values reported for the analytes on the PB modified electrode as compared with previous study. The mechanism in Scheme 1 was proposed for the electrocatalytic oxidation of NO_3^- at the EPPGE-SWCNT-PB electrode in aqueous solutions based on the previous reports on the mechanism of NO_3^- electro-oxidation at modified electrodes [38]:

The PB molecules on SWCNT platform consisted of the Fe^{2+}/Fe^{3+} catalyst which was electrochemically converted to its stable oxidation state as depicted in Eqn 6. The catalyst brings about nitrite ion oxidation thus producing NO_2 intermediates (Eqn 7). The intermediates were further oxidised to yield nitrate as the final product (Eqns 8 and 9), while the catalyst was regenerated on the electrode (Eqn 10).

$$[SWCNT\text{-}Fe^{3+}/Fe^{2+}]_{film} + H_2O \longrightarrow [SWCNT\text{-}Fe^{3+}/Fe^{3+}]_{film(aq)} + e^- \quad (6)$$

$$[SWCNT\text{-}Fe^{3+}/Fe^{3+}]_{film(aq)} + NO_2^- \rightleftharpoons [SWCNT\text{-}Fe^{3+}/Fe^{3+}]_{film} + NO_2 + e^- \ (slow) \quad (7)$$

$$2NO_2 + H_2O \rightleftharpoons 2H^+ + NO_3^- + NO_2^- \quad (8)$$

$$NO_2^- + H_2O \longrightarrow 2H^+ + NO_3^- + 2e^- \quad (9)$$

$$[SWCNT\text{-}Fe^{3+}/Fe^{3+}]_{film} + e^- \longrightarrow [SWCNT\text{-}Fe^{3+}/Fe^{2+}]_{film} \quad (10)$$

Scheme 1.

4.CONCLUSION

The study has described successfully the modification of EPPGE electrode with SWCNT/PB nanohybrids. The EPPGE-SWCNT-PB electrode was found to have better electron transport and catalytic efficiency towards the oxidation of nitrite and nitric oxide compared to the bare EPPGE and EPPGE-SWCNT electrodes. Electrocatalytic oxidation of nitrite at both pH studied indicated some

degree of adsorption of the analyte or its oxidation intermediates on the electrode. After electrochemical cleaning and re-use, the EPPGE-SWCNT-PB electrode gave current recovery of 85.0% and 93.7% due to the electro-catalytic oxidation of nitrite and nitric oxide respectively indicating that the adsorption process was dominantly physically induced. Despite the electrode kinetic limitation due to adsorption, its detection limit towards the analyte, its sensitivity and catalytic constant agreed favourably with values previously reported in literature.

ACKNOWLEDGEMENTS
This project was supported by the University of Johannesburg and the National Research Foundation. ASA thanks the University of Johannesburg for post-doctoral fellowship and Obafemi Awolowo University Nigeria for the research leave visit. We wish to thank Andrew and Chris of the microscopy laboratory, University of Pretoria, for acquiring the TEM and the FESEM images.

References

1. K. Zhao, H. Song, S. Zhuang, L. Dai, P. He, Y. Fang, *Electrochem. Commun.*, 9 (2007) 65.
2. A.L. Sousa, W.J.R. Santos, R.C.S. Luz, F.S. Damos, L.T. Kubota, A.A., Tanaka, S.M.C.N. Tanaka, *Talanta,* 75 (2008) 333.
3. D. Zheng, C. Hu, Y. Peng, S. Hu, *Electrochim. Acta, 54* (2009) 4910.
4. W.J.R. Santos , P.R. Lima , A.A. Tanaka , S.M.C.N. Tanaka, L.T. Kubota, *Food Chemistry,* 113 (2009) 1206.
5. P. Wang, Z. Mai, Z. Dai, Y. Li, X. Zou, *Biosens. Bioelectr.*, 24 (2009) 3242.
6. M.M.E. Duarte, M.M. Stefenel, C.E. Mayer, *J Arg Chem Soc.*, 90 (2002) 111.
7. A.S. Adekunle, J. Pillay, K.I. Ozoemena, *Electrochim. Acta,* 55 (2010) 4319.
8. S.Y. Ha, S. Kim, *J. Electroanal. Chem.*, 468 (1999) 131.
9. Z.H. Wen, T.F. Kang, *Talanta,* 62 (2004) 351.
10. C. E. Banks, R.G. Compton, *Analyst,* 131 (2006) 15.
11. C.E. Banks, R.G. Compton, *Analyst,* 130 (2005) 1232.
12. E.R. Lowe, C.E. Banks, R.G. Compton, *Anal. Bioanal. Chem.*, 382 (2005) 1169.
13. E.R. Lowe, C.E. Banks, R.G. Compton, *Electroanalysis,* 17 (2005) 1627.
14. F. Wantz, C.E. Banks, R.G. Compton, *Electroanalysis,* 17 (2005) 1529.
15. C.M. Welch, C.E. Banks, S. Komorsky-Lovric, *Croat. Chim. Acta,* (in press).
16. F. Wantz, C.E. Banks, R.G. Compton, *Electroanalysis,* 17 (2005) 655.
17. E. Bustos, Luis A. Godinez, Int. *J. Electrochem. Sci.,* 6 (2011) 1-36.
18. G. Selvarani, S.K. Prashant, A.K. Sahu, P. Sridhar, S. Pitchumani, A.K. Shukla, *J. Power Sources,* 178 (2008) 86-91.
19. D. Moscone, D. D'Ottavi, D. Compagnone, G. Palleschi, A. Amine, *Anal. Chem.*, 73 (2001) 2529.
20. S. Ijima, T. Ichihashi, *Nature,* 363 (1993) 603.
21. A.Salimi, A. Noorbakhash, F. S. Karonian. *Int. J. Electrochem. Sci.*, 1 (2006) 435.
22. Li Zhang, Zhen Fang, Guang-Chao Zhao and Xian-Wen Wei. *Int. J. Electrochem. Sci.*, 3 (2008) 746.
23. W. Frenzel, J. Schulz-Brussel, B. Zinvirt, *Talanta,* 64 (2004) 278.
24. M.I.H. Helaleh, T. Korenaga, *J. Chromatogr. B,* 744 (2000) 433.
25. S. Han, Y. Chen, R. Pang, P. Wan, *Ind. Eng. Chem. Res. 46* (2007) 6847.
26. A.S. Adekunle, K.I. Ozoemena, *Electroanalysis,* 22 (2010) 2519.
27. Y.-L. Hu, J.-H. Yuan, W. Chen, K. Wang, X.-H. Xia, *Electrochem. Commun.*, 7 (2005) 1252.

28. A.Ernst, O. Makowski, B. Kowalewska, K. Miecznikowski, P.J. Kulesza, *Bioelectrochem.*, 71 (2007) 23.
29. S. Vaucher, M. Li, S. Mann, *Angew. Chem. Int. Ed.*, 39 (2000) 1793.
30. A.J. Bard, L.R. Faulkner, Electrochemical Methods: Fundamentals and Applications, 2nd ed., John Wiley & Sons, Hoboken, NJ., 2001.
31. J.N. Soderberg, A.C. Co, A.H. C. Sirk, V.I. Birss, *J. Phys. Chem. B,* 110 (2006) 10401.
32. F. Matemadombo, T. Nyokong, *Electrochim. Acta*, 52 (2007) 6856.
33. Y. Shih, J.-M. Zen, A.S. Kumar, P-Y. Chen, Talanta, 62 (2004) 912.
34. G. D. Christian, Analytical Chemistry, 6th ed., Wiley, New York 2004, p. 113.
35. R. Ojani, J.-B., Raoof, E. Zarei, *Electrochim. Acta*, 52 (2006) 753.
36. N.S. Trofimova, A.Y. Safronov, O. Ikeda, *Electrochim. Acta*, 50 (2005) 4637.
37. H.X. Ju, L. Donal, *J. Electroanal. Chem*., 484 (2000) 150.
38. F. Armijo, M.C. Goya, M. Reina, M.J. Canales, M.C. Arevalo, M.J. Aguire, *J. Mol. Cat. A*: 268 (2007) 148.